

Thermoelectric property of a one dimensional channel in the presence of a transverse magnetic field

Cite as: Appl. Phys. Lett. **115**, 202102 (2019); <https://doi.org/10.1063/1.5128906>

Submitted: 23 September 2019 . Accepted: 29 October 2019 . Published Online: 11 November 2019

Chengyu Yan , Michael Pepper , Patrick See, Ian Farrer , David A. Ritchie, and Jonathan Griffiths

COLLECTIONS

 This paper was selected as an Editor's Pick



View Online



Export Citation



CrossMark

ARTICLES YOU MAY BE INTERESTED IN

[Flexible CoFeB/MgO-based magnetic tunnel junctions annealed at high temperature \(\$\geq 350^\circ\text{C}\$ \)](#)
Applied Physics Letters **115**, 202401 (2019); <https://doi.org/10.1063/1.5128952>

[Tunable high-quality Fano resonance in coupled terahertz whispering-gallery-mode resonators](#)
Applied Physics Letters **115**, 201102 (2019); <https://doi.org/10.1063/1.5129073>

[Tunable giant Rashba-type spin splitting in PtSe₂/MoSe₂ heterostructure](#)
Applied Physics Letters **115**, 203501 (2019); <https://doi.org/10.1063/1.5125303>



**THE WORLD'S RESOURCE FOR
VARIABLE TEMPERATURE
SOLID STATE CHARACTERIZATION**



WWW.MMR-TECH.COM

OPTICAL STUDIES SYSTEMS

SEEBECK STUDIES SYSTEMS

MICROPROBE STATIONS

HALL EFFECT STUDY SYSTEMS AND MAGNETS

Thermoelectric property of a one dimensional channel in the presence of a transverse magnetic field

Cite as: Appl. Phys. Lett. **115**, 202102 (2019); doi: [10.1063/1.5128906](https://doi.org/10.1063/1.5128906)

Submitted: 23 September 2019 · Accepted: 29 October 2019 ·

Published Online: 11 November 2019



View Online



Export Citation



CrossMark

Chengyu Yan,^{1,2,3,a)}  Michael Pepper,^{1,2}  Patrick See,⁴ Ian Farrer,⁵  David A. Ritchie,⁶ and Jonathan Griffiths⁶

AFFILIATIONS

¹London Centre for Nanotechnology, 17-19 Gordon Street, London WC1H 0AH, United Kingdom

²Department of Electronic and Electrical Engineering, University College London, Torrington Place, London WC1E 7JE, United Kingdom

³Micronova, Aalto University, Tietotie 3, Otaniemi, Espoo O2150, Finland

⁴National Physical Laboratory, Hampton Road, Teddington, Middlesex TW11 0LW, United Kingdom

⁵Department of Electronic and Electrical Engineering, University of Sheffield, Sheffield S1 3JD, United Kingdom

⁶Cavendish Laboratory, J.J. Thomson Avenue, Cambridge CB3 0HE, United Kingdom

^{a)}Electronic mail: uceeya3@ucl.ac.uk

ABSTRACT

We studied the thermal conduction through a quantum point contact (QPC), defined in a GaAs-Al_xGa_{1-x}As heterostructure, in the presence of a transverse magnetic field. A shift in the position of a thermo-voltage peak is observed with increasing field. The position of the thermo-voltage peak follows the Cutler-Mott relation in the small field regime ($B < 0.5$ T); it starts diverging from the Cutler-Mott relation in the moderate field regime, where a cubic magnetic field term dominates over the trivial quadratic term; eventually, the shift saturates in the large field regime ($B > 3.0$ T). Our results suggest that additional calibration is necessary when using QPC as thermometry, especially when the transverse magnetic field is applied.

© 2019 Author(s). All article content, except where otherwise noted, is licensed under a Creative Commons Attribution (CC BY) license (<http://creativecommons.org/licenses/by/4.0/>). <https://doi.org/10.1063/1.5128906>

Thermal and electric conduction, in a conducting system, are generally strongly coupled to each other, the mode that carries charge is the same one that carries energy (heat). The coupling is found to be well established in two-dimensional electron gas (2DEG) in both the low magnetic field and integer quantum Hall regime,¹⁻⁴ as well as one-dimensional electron gas.⁵⁻⁷ Some recent studies on the fractional quantum Hall regime (FQHE), where electron-electron interaction dominates, show different results regarding thermal conduction.⁸⁻¹¹ In all these works, quantum point contacts (QPCs) or quantum dots (QDs) have been widely employed to probe the local temperature and reveal the heat flow through the system. However, the role of QPCs or QDs in terms of heat flow has not been well characterized, especially in the presence of a transverse magnetic field.

In the present work, we focus on the impact of a transverse magnetic field on thermal conduction through a QPC. It is noticed the observations are well captured by the Cutler-Mott relation at zero field; however, a noticeable discrepancy between the Cutler-Mott relation

and experimental results occurs at a finite magnetic field. A cubic magnetic field term, in terms of the position of the thermovoltage peaks, dominates over the trivial quadratic term with a moderate magnetic field. Meanwhile, an anomalous lattice temperature dependence associated with the field is also revealed. Our results suggest that additional calibration is necessary when using QPC as thermometry.

The thermoelectric property of a system is closely associated with a thermal gradient across the system. In the experiment setup (see note 1 of [supplementary material](#) for the detailed setup) shown in [Fig. 1\(a\)](#), the whole system consists of three sections, once the split gates that define the quantum point contacts (QPCs) deplete electrons underneath the gates, namely the large 2DEG area with temperature T_0 , and the relatively small area enclosed by QPC1 (QPC2) with temperature T_1 (T_2). The QPCs serve as a thermal valve and local thermometry.^{6,7,12} A heating current I_H (at frequency f_0 , 33 Hz; 1 μ A) is fed to the 2DEG to increase T_0 . Since $T_0 > T_{1,2}$, a thermovoltage V_{th} is built between the large and small areas (measured at $2f_0$, because

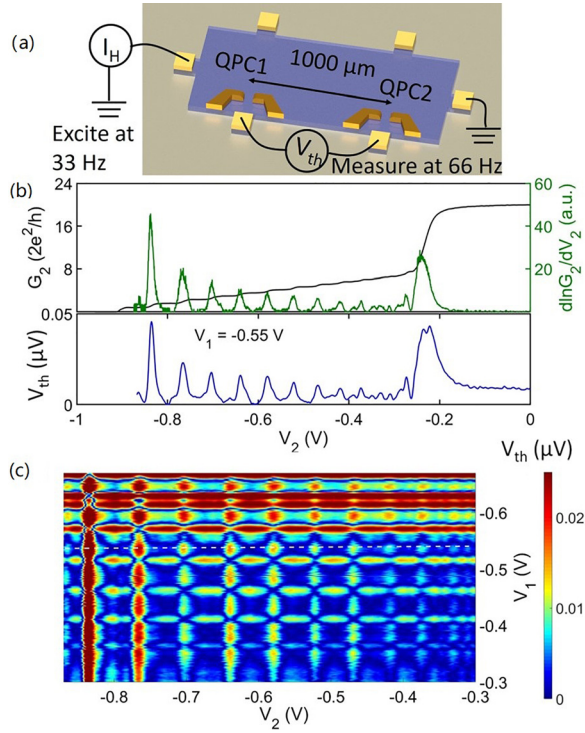


FIG. 1. Experimental setup and thermovoltage at zero magnetic field. (a) Schematic of the experimental setup. The squares at the edge of the mesa are Ohmic contacts. The shining metallic gates define QPC1 and 2, and the QPCs are separated by $\sim 1000 \mu\text{m}$. The large separation ensures that the coupling between the two QPCs is negligible. The schematic is not to scale. (b) The upper panel shows the conductance characteristic of QPC2. The lower panel illustrates representative results of V_{th} as a function of V_2 with QPC1 set to $3G_0$ ($G_0 = \frac{2e^2}{h}$). (c) V_{th} spectrum with both QPC1 and QPC2 set to quasi-1D regime ($V_1, V_2 \leq -0.3 \text{ V}$). The white dashed cut corresponds to results in (b).

heating power $P \propto I_H^2 R$. V_{th} depends on the conductance of the QPCs, it vanishes if the QPCs are transparent (i.e., the QPCs are set to $n \times \frac{2e^2}{h}$, n is an integer), otherwise it takes a finite value. This behavior is well characterized by the Cutler-Mott relation^{13,14}

$$\frac{V_{th,i}}{T_i - T_0} = -\frac{\pi^2 k_B}{3e} (T_i + T_0) \frac{\partial \ln G_i}{\partial \mu_i}, \quad (1)$$

where $V_{th,i}$ is the thermovoltage between the i th QPC and common 2DEG, k_B is the Boltzmann constant, e is the elementary electron charge, G_i is the electric conductance of the i th QPC, and μ_i is the chemical potential within the QPCs. It is necessary to comment that the usage of two QPCs minimizes the effect due to temperature fluctuation in the large 2DEG region.^{7,12} As a result, we focus on the net thermo-voltage drop between the two small area $V_{th} = V_{th,1} - V_{th,2}$. However, most of the results can be obtained with a single-QPC setup.

Figure 1(b) demonstrates the excellent agreement between the Cutler-Mott relation (upper panel) and measured V_{th} (lower panel), which can be used to calibrate the system. The thermo-voltage was recorded by sweeping gate voltage applied to QPC2 whereas QPC1 was set to $3G_0$. Tuning V_1 and V_2 (gate voltage applied to QPC1 and 2) independently, we could extract a detailed V_{th} spectrum, as

illustrated in Fig. 1(c). Well organized patterns were observed. The bright horizontal segments happened when QPC2 was transparent, and QPC1 was not; vice versa for the vertical segments. The dark square region corresponded to the situation when both QPC1 and QPC2 were transparent. A complete spectrum, including the 2D regime, can be found in [supplementary material](#), Fig. S1.

After calibrating the measurement system at zero magnetic field, a transverse magnetic field B_{\perp} was applied to the sample. B_{\perp} is expected to influence the thermal property of the system because it affects the electron cooling and heat generation processes. At zero field, the temperature reaches maximal at the center of the sample and then decreases to reach the lattice temperature at the contacts; in the presence of a transverse magnetic field, the heat is generated when the edge channels connect to the contacts, creating two hot spots close to each contact and located on opposite sides (top and bottom) of the sample.¹⁵

It is necessary to comment that the position of the thermovoltage peak with respect to gate voltage V_i is mainly determined by the i th QPC within the range of magnetic field in the present work. Using a single QPC or double QPCs leads to a similar result, as illustrated in Fig. S1. On the other hand, the amplitude of the peak could be sensitive to the arrangement of the QPCs. For instance, the amplitude of the thermovoltage peak with the QPCs located at the same edge may differ from that with the QPCs located at the opposite edges.

Here, we present a detailed magnetic field dependence of trace in Fig. 1(b) (i.e., QPC1 is set to $3G_0$ at zero field). It was found that the field had a twofold impact, as demonstrated in Fig. 2: first, the magnitude of V_{th} peaks was enhanced noticeably by B_{\perp} , which is consistent with the predicted increase in thermopower (hence thermovoltage) if

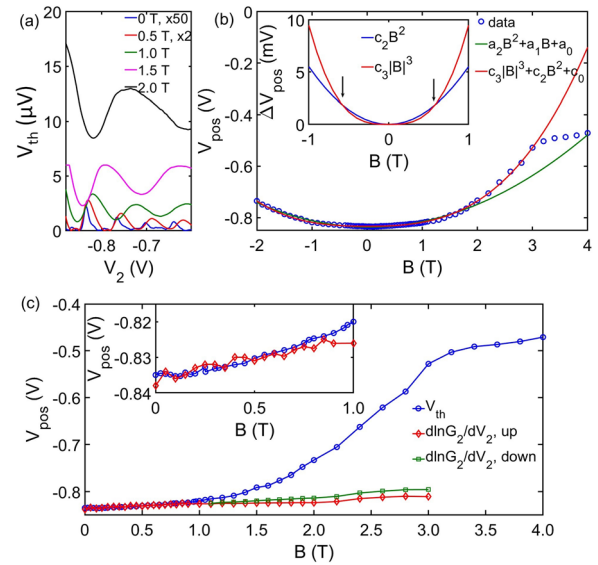


FIG. 2. Magnetic field dependence of the V_{th} peak position. (a) Trace in Fig. 1(b) as a function of transverse magnetic field ($G_1 = 3G_0$). A shift of position of V_{th} peaks, denoted as V_{pos} . (b) Position of the highlighted V_{th} peak in (a) (with respect to V_2). Solid traces show two types of fitting with (red) and without (green) $|B|^3$ term, respectively. The inset highlights contribution to peak shift from B^2 and $|B|^3$ terms. (c) Comparison between the measured V_{th} peak position and prediction based on $\frac{d \ln G_2}{dV_2}$. The inset shows a zoom-in of the low field regime.

size quantization owing to QPC is strong;¹⁶ this enhancement is also related to the fact the hot spot moves toward the edge of the sample; second and more important, a shift in the position of V_{th} peaks was introduced by B_{\perp} as shown in Figs. 2(a) and 2(b) [also supplementary material, Fig. S2]. The position of the V_{th} peak changed rapidly when $-3 \text{ T} < B_{\perp} < 3 \text{ T}$, and then saturated (when the bulk Landau filling factor approaches $\nu = 2$). The peak position follows such a relation $V_{pos} = c_3|B|^3 + c_2B^2 + c_0$ [red solid trace in Fig. 3(b)]. The B^2 term dominated in a small field regime whereas $|B|^3$ became the leading factor when $B_{\perp} \geq 0.5 \text{ T}$. In addition, it was also noticed that the V_{th} peak position agreed well with that predicted by $\frac{\partial \ln G_2}{\partial V_2}$ (i.e., Cutler-Mott relation) in small field ($B_{\perp} < 0.6 \text{ T}$); however, it diverged significantly from

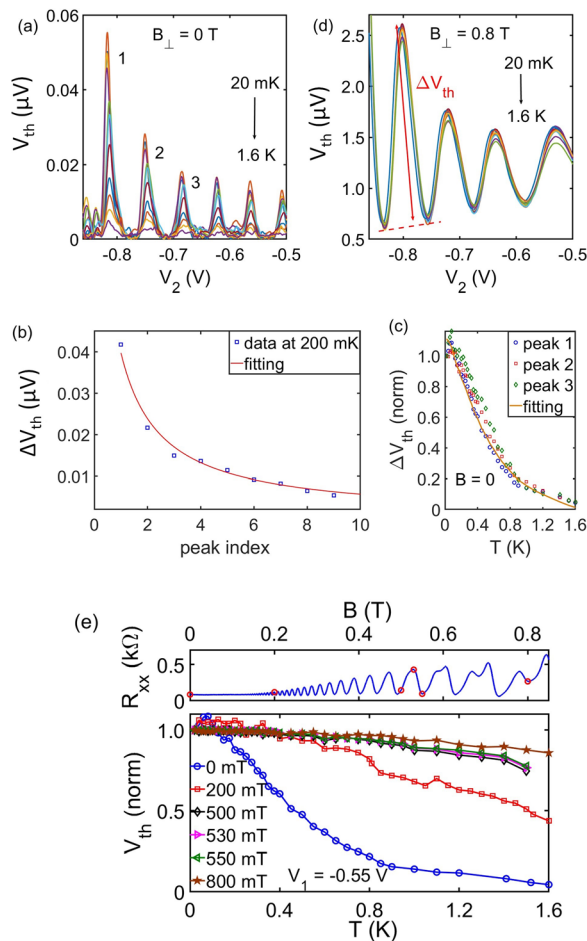


FIG. 3. Lattice temperature dependence of V_{th} peaks. (a) Temperature dependence at zero field. (b) Fitting of δV_{th} against the peak index at 200 mK at zero field. (c) Universal scaling behavior. (d) Temperature dependence at $B_{\perp} = 0.8 \text{ T}$. (e) The upper panel shows the SdH oscillation of the raw 2DEG. The red dots highlight the magnetic field values presented in the lower panel. The normalized magnitude of V_{th} peak 1, the highlighted peak in Fig. 2(a) [it occurs at different V_2 with increasing B_{\perp}], at the different magnetic field as a function of lattice temperature ranging from 20 mK to 1.6 K. The measured results at higher temperature are normalized against that at 20 mK.

the prediction in a large field regime [Fig. 2(c)]. Besides, $\frac{\partial \ln G_2}{\partial V_2}$ splits into two spin-resolved branches with increasing field due to Zeeman splitting whereas there was no sign of such splitting in the V_{th} peak.

In principle, both V_{th} and $\frac{\partial \ln G_2}{\partial V_2}$ monitor the position of the 1D subbands within the QPC, which determine the heat and charge transport through the QPC. The fact that V_{th} peak correlates with $\frac{\partial \ln G_2}{\partial V_2}$ in a small field regime where B^2 dominated indicates that the B^2 term arises from magnetic depopulation induced 1D subband rearrangement.^{17,18} The origin of the $|B|^3$ term, on the other hand, was unclear. Higher-order B dependence can be induced if the electrostatic confinement is not parabolic, for instance, due to disorder;¹⁷ however, the impact of nonparabolic confinement should also be revealed in electrical measurement $\frac{\partial \ln G_2}{\partial V_2}$. Besides, the parabolicity of electrostatic confinement is double-checked by fitting the conductance to the saddle point model [Note 2 and Fig. S3 of supplementary material]. Therefore, the $|B|^3$ term is a unique characteristic of heat transport.

Anomalous temperature dependence associated with the magnetic field was also observed, as shown in Fig. 3 (see note 3 of the supplementary material for details on the fitting). It was found that the magnitude of the thermovoltage peak attenuated rapidly with increasing lattice temperature at low magnetic field similar to the previous report^{7,12} as seen in Fig. 3(a), and exhibited a universal scaling [Figs. 3(b) and 3(c)]; on the other hand, it was rather insensitive to temperature changes in the regime where $|B|^3$ term dominates, as exemplified by results at $B = 0.8 \text{ T}$ in Fig. 3(d). It is intuitive to think that the observed temperature might be relevant with the edge channels because the QPC is attached to the hot spot near the Ohmic contact via the medium of edge channels. This scenario is somehow not supported by the data shown in Fig. 3(e). It is particularly interesting to note V_{th} obtained at 500 (Shubnikov-de Haas dip), 530 (peak), and 550 mT (dip) showed similar behavior, whereas it was well known that electrical measurements at SdH dip and peak had rather distinguishable temperature dependence.^{19–21}

The results at zero magnetic field can be well described by the Cutler-Mott relation, which is a single-electron framework. Our results suggest that this framework does not hold in the presence of a finite transverse magnetic field. It is helpful to discuss several mechanisms beyond single-electron frameworks which are known to affect thermal conduction:

- I. Phonon drag augments thermopower (also thermovoltage) with increasing magnetic field.^{22,23} However, phonon drag usually freezes out below 0.6 K in the GaAs heterojunction.²³ In our experiment, there was no sign of phonon drag switching on/off at the finite magnetic field.
- II. A spin density wave (SDW) can be induced by a transverse magnetic field,^{24–27} and it is separated from the single-particle mode by an energy gap.^{28,29} The melting temperature of an SDW is enhanced by the magnetic field,^{26,30} which might result in the observed evolution in temperature dependence. However, observations on an SDW in GaAs heterojunctions usually involve excitation between several 2D subbands,^{28,29} which is unlikely to be found in the current experiment.
- III. It is known that e-e interaction can make thermal conduction of a 1D system diverge from the Cutler-Mott relation, such as the finite thermopower at 0.7 conductance anomaly.^{7,31} However, a detailed theory on QPC-mediated thermal

conduction that incorporates electron-electron interaction, especially in the presence of a transverse magnetic field, is lacking. More specifically, it is difficult to comment at the moment why the e-e interaction prevents the occurrence of spin splitting in V_{th} .

In conclusion, we have observed unexplained thermal conduction through a 1D channel in the presence of a transverse magnetic field. The magnetic field and temperature dependence indicate that the thermal conduction at the finite magnetic field is beyond the single-particle picture. The results are important when employing the QPC to probe energy flow in integer/fractional quantum Hall or other exotic systems, where the magnetic field plays an important role.

See the [supplementary material](#) for the results under different experimental conditions and details on the fitting of temperature dependence data.

The authors gratefully acknowledge fruitful discussions with Karl-Fredrik Berggren, Kalarikad Thomas, and James Nicholls. The work was funded by the United Kingdom Research and Innovation (UKRI).

REFERENCES

- ¹C. Possanzini, R. Fletcher, P. T. Coleridge, Y. Feng, R. L. Williams, and J. C. Maan, "Diffusion thermopower of a two-dimensional hole gas in SiGe in a quantum Hall insulating state," *Phys. Rev. Lett.* **90**, 176601 (2003).
- ²C. Possanzini, R. Fletcher, M. Tsaousidou, P. T. Coleridge, R. L. Williams, Y. Feng, and J. C. Maan, "Thermopower of a p-type Si/Si_{1-x}Ge_x heterostructure," *Phys. Rev. B* **69**, 195306 (2004).
- ³Y. M. Zuev, W. Chang, and P. Kim, "Thermoelectric and magnetothermoelectric transport measurements of graphene," *Phys. Rev. Lett.* **102**, 096807 (2009).
- ⁴G. Granger, J. P. Eisenstein, and J. L. Reno, "Observation of chiral heat transport in the quantum Hall regime," *Phys. Rev. Lett.* **102**, 086803 (2009).
- ⁵P. Streda, "Quantised thermopower of a channel in the ballistic regime," *J. Phys.: Condens. Matter* **1**, 1025–1027 (1989).
- ⁶L. W. Molenkamp, H. Van Houten, C. W. J. Beenakker, R. Eppenga, and C. T. Foxon, "Quantum oscillations in the transverse voltage of a channel in the nonlinear transport regime," *Phys. Rev. Lett.* **65**, 1052–1055 (1990).
- ⁷N. J. Appleyard, J. T. Nicholls, M. Pepper, W. R. Tribe, M. Y. Simmons, and D. A. Ritchie, "Direction-resolved transport and possible many-body effects in one-dimensional thermopower," *Phys. Rev. B* **62**, R16275–R16278 (2000).
- ⁸C. L. Kane, M. P. A. Fisher, and J. Polchinski, "Randomness at the edge: Theory of quantum Hall transport at filling $\nu = 2/3$," *Phys. Rev. Lett.* **72**, 4129–4132 (1994).
- ⁹A. Bid, N. Ofek, H. Inoue, M. Heiblum, C. L. Kane, V. Umansky, and D. Mahalu, "Observation of neutral modes in the fractional quantum Hall regime," *Nature* **466**, 585 (2010).
- ¹⁰M. Goldstein and Y. Gefen, "Suppression of interference in quantum Hall Mach-Zehnder geometry by upstream neutral modes," *Phys. Rev. Lett.* **117**, 276804 (2016).
- ¹¹R. Sabo, I. Gurman, A. Rosenblatt, F. Lafont, D. Banitt, J. Park, M. Heiblum, Y. Gefen, V. Umansky, and D. Mahalu, "Edge reconstruction in fractional quantum Hall states," *Nat. Phys.* **13**, 491 (2017).
- ¹²N. J. Appleyard, J. T. Nicholls, M. Y. Simmons, W. R. Tribe, and M. Pepper, "Thermometer for the 2D electron gas using 1D thermopower," *Phys. Rev. Lett.* **81**, 3491–3494 (1998).
- ¹³M. Cutler and N. F. Mott, "Observation of Anderson localization in an electron gas," *Phys. Rev.* **181**, 1336–1340 (1969).
- ¹⁴U. Sivan and Y. Imry, "Multichannel Landauer formula for thermoelectric transport with application to thermopower near the mobility edge," *Phys. Rev. B* **33**, 551–558 (1986).
- ¹⁵U. Klass, W. Dietsche, K. von Klitzing, and K. Ploog, "Imaging of the dissipation in quantum-Hall-effect experiments," *Z. Phys. B* **82**, 351–354 (1991).
- ¹⁶V. A. Margulis and A. V. Shorokhov, "Thermopower of two-dimensional channels and quantum point contacts in a magnetic field," *J. Phys.: Condens. Matter* **15**, 4181–4188 (2003).
- ¹⁷K. F. Berggren, T. J. Thornton, D. J. Newson, and M. Pepper, "Magnetic depopulation of 1D subbands in a narrow 2D electron gas in a GaAs:AlGaAs heterostructure," *Phys. Rev. Lett.* **57**, 1769–1772 (1986).
- ¹⁸B. J. van Wees, L. P. Kouwenhoven, E. M. M. Willems, C. J. P. M. Harmans, J. E. Mooij, H. Van Houten, C. W. J. Beenakker, J. G. Williamson, and C. T. Foxon, "Quantum ballistic and adiabatic electron transport studied with quantum point contacts," *Phys. Rev. B* **43**, 12431–12453 (1991).
- ¹⁹H. P. Wei, A. M. Chang, D. C. Tsui, and M. Razeghi, "Temperature dependence of the quantized Hall effect," *Phys. Rev. B* **32**, 7016–7019 (1985).
- ²⁰M. P. Lilly, K. B. Cooper, J. P. Eisenstein, L. N. Pfeiffer, and K. W. West, "Evidence for an anisotropic state of two-dimensional electrons in high Landau levels," *Phys. Rev. Lett.* **82**, 394–397 (1999).
- ²¹Y. Zhang, Y. Tan, H. L. Stormer, and P. Kim, "Experimental observation of the quantum Hall effect and Berry's phase in graphene," *Nature* **438**, 201 (2005).
- ²²R. Fletcher, M. D'orio, A. S. Sachrajda, R. Stoner, C. T. Foxon, and J. J. Harris, "Evidence of phonon drag in the thermopower of a GaAs-Ga_{0.68}Al_{0.32} As heterostructure," *Phys. Rev. B* **37**, 3137–3140 (1988).
- ²³C. Ruf, H. Obloh, B. Junge, E. Gmelin, K. Ploog, and G. Weimann, "Phonon-drag effect in GaAs-Al_xGa_{1-x} As heterostructures at very low temperatures," *Phys. Rev. B* **37**, 6377–6380 (1988).
- ²⁴D. Yoshioka and P. A. Lee, "Ground-state energy of a two-dimensional charge-density-wave state in a strong magnetic field," *Phys. Rev. B* **27**, 4986–4996 (1983).
- ²⁵J. F. Kwak, J. E. Schirber, P. M. Chaikin, J. M. Williams, H. H. Wang, and L. Y. Chiang, "Spin-density-wave transitions in a magnetic field," *Phys. Rev. Lett.* **56**, 972–975 (1986).
- ²⁶N. J. Naughton, R. V. Chamberlin, X. Yan, S. Y. Hsu, L. Y. Chiang, M. Ya Azbel, and P. M. Chaikin, "Reentrant field-induced spin-density-wave transitions," *Phys. Rev. Lett.* **61**, 621–624 (1988).
- ²⁷A. A. Koulakov, M. M. Fogler, and B. I. Shklovskii, "Charge density wave in two-dimensional electron liquid in weak magnetic field," *Phys. Rev. Lett.* **76**, 499–502 (1996).
- ²⁸A. Pinczuk, S. Schmitt-Rink, G. Danan, J. P. Valladares, L. N. Pfeiffer, and K. W. West, "Large exchange interactions in the electron gas of GaAs quantum wells," *Phys. Rev. Lett.* **63**, 1633–1636 (1989).
- ²⁹A. Schmeller, A. R. Goni, A. Pinczuk, J. S. Weiner, J. M. Calleja, B. S. Dennis, L. N. Pfeiffer, and K. W. West, "Inelastic light scattering by spin-density, charge-density, and single-particle excitations in GaAs quantum wires," *Phys. Rev. B* **49**, 14778–14781 (1994).
- ³⁰R. C. Yu, L. Chiang, R. Upasani, and P. M. Chaikin, "Magnetothermopower of (TMTSF)₂ClO₄ and a new high-field phase," *Phys. Rev. Lett.* **65**, 2458–2461 (1990).
- ³¹B. Brun, F. Martins, S. Faniel, A. Cavanna, C. Ulysse, A. Ouerghi, U. Gennser, D. Mailly, P. Simon, S. Huang, and M. Sanquer, "Thermoelectric scanning-gate interferometry on a quantum point contact," *Phys. Rev. Appl.* **11**, 034069 (2019).